IOPscience iopscience.iop.org

Home Search Collections Journals About Contact us My IOPscience

Study of the structure of porous silicon via positron annihilation experiments

This article has been downloaded from IOPscience. Please scroll down to see the full text article.

2000 J. Phys.: Condens. Matter 12 5961

(http://iopscience.iop.org/0953-8984/12/27/314)

View the table of contents for this issue, or go to the journal homepage for more

Download details:
IP Address: 171.66.16.221
The article was downloaded on 16/05/2010 at 05:19

Please note that terms and conditions apply.

J. Phys.: Condens. Matter **12** (2000) 5961–5970. Printed in the UK PII: S0953-8984(00)12054-5

Study of the structure of porous silicon via positron annihilation experiments

M Biasini†§, G Ferro†§, M A Monge†‖, G Di Francia‡ and V La Ferrara‡
† ENEA, via don Fiammelli 2, 40129 Bologna, Italy
‡ ENEA, via Vecchio Macello, 80055 Portici, Italy

Received 25 February 2000, in final form 3 May 2000

Abstract. We performed two-dimensional angular correlation of the electron–positron annihilation radiation (2D-ACAR) and positron lifetime measurements on a porous Si sample. From the width of the narrow 2D-ACAR component, attributed to the positronium atom, we estimated the average size of the pores to be ∼2.4 nm and did not find evidence of a preferential propagation of the pores. Moreover, by comparing the 2D-ACAR spectrum with that observed for a pure Si crystal, we isolated a further isotropic component attributable to crystal defects of unknown origin.

1. Introduction

The strong-photoluminescence (PL) properties of porous silicon (PS), produced by electro-etching crystalline Si in hydrofluoric acid (HF) solution, have been the subjects of extensive studies in the last decade. Bulk crystalline Si (c-Si) has a relatively small energy gap (1.1 eV at room temperature, corresponding to near-infrared light) which allows visible light absorption via electron–hole production. However, due to momentum conservation, the process of light emission via electron–hole recombination needs to be phonon assisted, competing unfavourably with non-radiative decays. Conversely, the absorption edge of PS is shifted toward the blue [1, 2] and its radiative recombination properties are $\sim 10^5$ times more efficient. The most widely accepted explanation for such properties is based on quantum-size effects: the nanowires which result from the etching process, of typical size q, increase the energy gap which determines the absorption threshold by an amount ΔE of the order of

$$\Delta E = \frac{\hbar^2}{2m^*}\left(\frac{2\pi}{q}\right)^2 \tag{1}$$

where $\hbar$ is Planck's constant and m^* is the effective mass of the carrier (electron or hole). Moreover, although the underlying mechanism is not entirely understood, it is generally accepted that the efficient radiative recombination and consequent PL of PS is due to a relaxation of the $\boldsymbol{k}$-selection rules through the Heisenberg uncertainty principle. The PL light undergoes then a reduced absorption due to the increase of the energy gap. However, other models, ascribing the PL process to surface passivation, radiative surface states or molecular electronics, based on the fluorescence properties of Si–O–H compounds derived from siloxene ($Si_6O_3H_6$), are currently under discussion [3–5]. To understand the underlying mechanism which determines the PL properties of PS, of interest in view of the use in optoelectronic

§ Istituto Nazionale di Fisica della Materia.
‖ Permanent address: Universidad Carlos III, Avenida Universidad 30, Leganes (Madrid), 28911, Spain.

0953-8984/00/275961+10$30.00 © 2000 IOP Publishing Ltd

devices, investigations of the microscopic structure by transmission electron microscopy (TEM), scanning tunnelling microscopy, Auger spectroscopy, Raman spectroscopy, small-angle x-ray or neutron scattering (SAXS, SANS) and positron annihilation spectroscopy (PAS) were utilized. A serious problem with the traditional TEM sample preparation is the potential damage to the fragile PS structure. On the other hand, PAS is non-destructive and particularly suited to the study of bulk or surface defects linked to the pores. Experiments based on positron lifetime measurements [6] confirmed the sensitivity of PAS to the pores, monitoring the formation of positronium (Ps†), but did not produce quantitative results on the PS topology [7–10].

Previous 2D-ACAR studies yielded a radially averaged estimate of the porous structures [11, 12] but did not exploit the full power of the 2D-ACAR experiment, which is suitable for studying the anisotropic properties of the electron–positron momentum density. Indeed, a 2D-ACAR experiment, by measuring the distribution $N(\theta_x, \theta_y)$ of the angles of deviation from anticollinearity of the annihilation γ-rays, determines a two-dimensional projection, $\rho_{2D}^{2\gamma}(p_x, p_y)$, of the two-photon electron–positron momentum density, $\rho^{2\gamma}(\boldsymbol{p})$:

$$N(\theta_x, \theta_y) = \text{constant} \times \rho_{2D}^{2\gamma}(p_x, p_y) = \text{constant} \times \int_{-\infty}^{\infty} \rho^{2\gamma}(\boldsymbol{p})\, \mathrm{d}p_z. \tag{2}$$

In the independent-particle model (IPM), $\rho^{2\gamma}(\boldsymbol{p})$ can be expressed in atomic units as

$$\rho^{2\gamma}(\boldsymbol{p}) = \text{constant} \times \sum_{n,\boldsymbol{k}}^{occ} \left| \int \exp(-\mathrm{i}\boldsymbol{p}\cdot\boldsymbol{r}) \psi_{\boldsymbol{k}}^{n}(\boldsymbol{r}) \phi(\boldsymbol{r})\, \mathrm{d}\boldsymbol{r} \right|^2. \tag{3}$$

Here $\psi_{\boldsymbol{k}}^{n}$ and ϕ denote the $\boldsymbol{k}$-electron and positron wave functions, respectively, and the summation extends over all occupied $\boldsymbol{k}$-electron states from bands of index n [13–15]. Although this experiment was mainly used for electronic structure studies on perfect crystalline metals and semiconductors, it was established that a careful analysis of $\rho^{2\gamma}(\boldsymbol{p})$ could yield relevant information on vacancy-like defects in semiconductors [16]. Moreover, from the width of the momentum density of the centre of mass of the Ps atom, observed to form in voids in metals and semiconductors, one can obtain, via the uncertainty principle, quantitative information on the sizes of extended open-volume defects [17].

In this paper we perform a full two-dimensional analysis of the 2D-ACAR data and complement the results with positron lifetime experiments. We separate out a narrow distribution, attributable to the momentum density of the centre of mass of para-positronium, from which we estimate the sizes of the porous structures. Moreover we isolate a broad isotropic component attributable to defect structures not related to surface states. Possible explanations of the natures of these defects and their implications for PL properties are discussed.

2. Experiment

The PS was obtained by electrochemical etching of a 1 Ω cm, n-type-silicon Czochralski-zone wafer with a current density 40 mA cm^{-2} under exposure to the light of a 250 W Hg lamp [2]. The current direction was normal to the wafer plane and parallel to the [100] crystal axis. The etching solution was prepared by adding a 30% volume of isopropyl alcohol to a 70% volume of an HF aqueous solution (50% by weight). The current density and etching time were adjusted to obtain ∼50 μm thick layers of ∼45% porosity. A gravimetric method was used for the porosity measurements and a step profiler for the thickness determination. After production, PS samples were rinsed in pentane (low vapour pressure) to avoid superficial cracks and then

† Please note the difference between the acronyms Ps (positronium) and PS (porous silicon).

cut to obtain 1 cm^2 areas. The PL measurements were carried out using as the excitation source the 442 nm line of a HeCd laser. The power incident on the sample was always 1 mW cm^{-2}. A monochromator blazed at 500 nm and a charge-coupled-device detector were used to collect the PL spectra.

Figure 1 shows the typical PL spectrum for the PS sample *as produced* and after immersion in a bath of 10% HF solution. It can be noted that the centroid of the PL peak was shifted to a slightly higher energy by the immersion in the HF bath. According to the quantum confinement model, this shift should be due to the thinning of the nanowires caused by the partial removal of the superficial oxide layer.

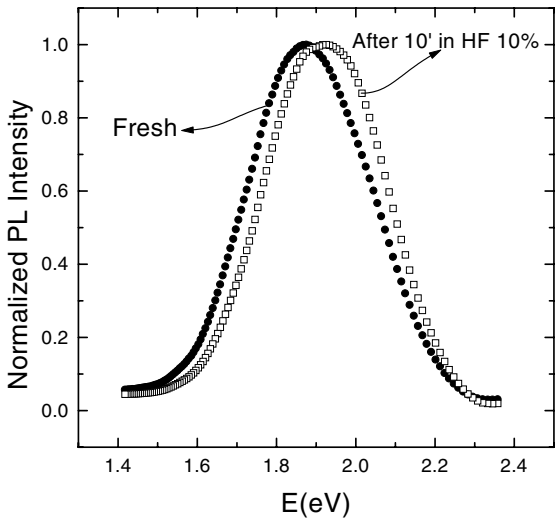

Figure 1. PL spectra produced by the PS *as produced* and after 10 minutes in 10% HF solution.

The PS sample showed distinct x-ray diffraction spots in a Von Laue experiment. As the thickness of the porous layer ($\sim$50 μm) was of the same order as the average penetration of the x-ray beam in Si ($\sim$100 μm), this finding suggests that the HF treatment did not produce an amorphous phase in the porous layer [18]. Indeed, the diffraction pattern was identical and as intense as that displayed by the 550 μm thick n-type c-Si which was used to produce the porous Si sample (space group $Fd3m$).

The 2D-ACAR experiments were carried out on a system based on a pair of Anger cameras [19]. Each detector comprised a 42 cm diameter, 1.25 cm thick Na(I) crystal scintillator, optically coupled to a close-packed honeycomb array of 61 photomultipliers. An 11 m sample–detector distance provided a coincidence angular view of 37.4×37.4 $mrad^2$ (one milliradian is equivalent to 0.137 momentum au) in a 256×256 matrix. At this distance the 'optical' angular resolution was 0.57 mrad. The resolving coincidence time for the photon pair selection was 60 ns. A 2 T water-cooled electromagnet was employed to focus the positrons, emitted by a 1.85×10^9 Bq intense ^{22}Na source, onto the sample. The estimated overall experimental resolution, obtained by combining the optical resolution with the intrinsic sizes of the positron source spot at the sample and the thermal motion of the positron ($\sim$0.22 mrad at 55 K and $\sim$0.54 mrad at 300 K), was (0.58, 0.95) mrad at 55 K and (0.8, 1.07) mrad at 300 K for the p_x- and p_y-directions, respectively. A tungsten collimator shielded the detectors from the radiation not emitted directly from the sample. The PS and c-Si samples were positioned on a microgoniometer, part of the sample holder, and oriented, via a preliminary

Von Laue diffraction experiment, with the $[0\bar{1}1]$ crystal direction parallel to the main axis of the spectrometer, which selects the average integration direction. The p_x- and p_y-directions of the detector plane were parallel to the [100] and [011] crystal axes, respectively. Whereas the spectrum for the c-Si contained $\sim 2 \times 10^8$ raw coincidence counts, several acquisitions under different conditions were carried out for the porous Si, amounting to an overall $\sim 2.5 \times 10^8$ raw coincidence counts. The measurements were carried out at room temperature and at $\sim$55 K, in a vacuum of $\sim 10^{-6}$ mbar. The 'raw' spectra were subsequently corrected with the so-called momentum-sampling function, which removes the distortions resulting from spatial variations in the single-detector efficiencies and the finite apertures of those detectors [19].

Positron lifetime experiments were performed with a fast–fast lifetime set-up with barium fluoride (BaF_2) scintillators having a time resolution of 185 ps. The ^{22}Na positron source (3.5×10^5 Bq) was deposited between two 7.5 μm thick Kapton foils and sandwiched with a pair of samples. The system was thermostated within 1 °C. The spectra, amounting to $\sim 5 \times 10^6$ coincidence counts, were analysed by means of the PATFIT program [20] as sums of three exponential decays, after background and source subtraction. The lifetime measurements were performed at room temperature for the following thermal and pressure configurations:

(i) at atmospheric pressure;
(ii) at atmospheric pressure after immersion in a bath of 10% HF solution;
(iii) in a vacuum of 10^{-4} mbar after a three-hour-long thermal annealing at 800 °C at a pressure of 5×10^{-5} mbar.

3. Results and discussion

The results of the lifetime experiments, after subtraction of the contribution from the source, are reported in table 1.

Table 1. Results of the lifetime experiments for the conditions listed as points (i), (ii) and (iii) of section 2. The τ_b-value is obtained neglecting the third lifetime component..

Condition	τ_1 (ps)	I_1 (%)	τ_2 (ps)	I_2 (%)	τ_3 (ps)	I_3 (%)	τ_b (ps)
(i)	193 ± 2	66.1 ± 1	395 ± 6	32.4 ± 1	2847 ± 40	1.6 ± 0.1	234.5 ± 0.5
(ii)	190 ± 2	72.8 ± 1	361 ± 3	26.3 ± 1	2540 ± 40	0.9 ± 0.1	219.0 ± 0.3
(iii)	179 ± 1	74.4 ± 1	397 ± 6	24.7 ± 1	1700 ± 70	0.9 ± 0.1	210.0 ± 0.5

In all cases a satisfactory fit was attained by a decomposition into three components (reduced $\chi^2 \sim 1$). It can be noted that the results of the decomposition analysis are almost independent of treatments (ii) and (iii), aimed at removing eventual surface positron traps, particularly the SiO_2 surface layer. This finding indicates that neither of the two short-lifetime components is related to the surface state. On the other hand, table 1 shows that the application of the simple two-state trapping model (neglecting the third component of very low intensity) [6] yields a bulk positron lifetime τ_b rather close to what is expected for c-Si (215–220 ps). This result, together with the preliminary Von Laue experiment mentioned in section 2, suggests that a relevant fraction f_b of the positrons annihilate in the columnar structures and in the substrate from the delocalized (bulk) state. The standard trapping model yields $f_b \sim 0.85$. Indeed, τ_1 is probably a combination of τ_b, for annihilations in the defect-free substrate, and a short lifetime due to annihilations from a delocalized state in the porous layer plus escape in the columnar defects. However, a decomposition into four exponential decays (after source subtraction) did not significantly improve the reduced χ^2 and the results of the fit were quite

erratic. The third-component value is typical for annihilation of ortho-positronium via 'pick-off', although it is smaller than those reported from other lifetime experiments on porous Si [7–9]. Figure 2 shows the central part of the 2D-ACAR spectrum of PS at 55 K compared to the spectrum of c-Si, normalized to the same number of counts, at the same temperature. The anisotropic structures of the two spectra (for $p \geqslant 2$ mrad) are almost identical and are consistent with previous experiments on c-Si and c-Ge for the same projections [19,21,22]. The main features of the momentum distribution of c-Si were described with reasonable accuracy by Chiba and Akahane [21] within the framework of the linear combination of atomic orbitals (LCAO) formalism. The basis chosen was s and p orbitals of two ions in the unit cell forming covalent bonding.

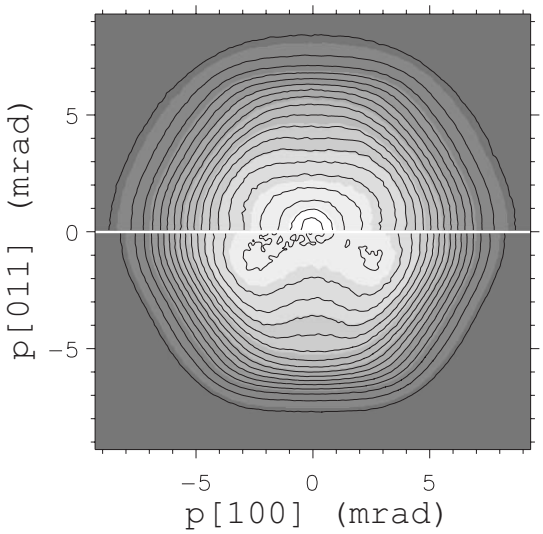

Figure 2. The central part of the 2D-ACAR spectrum of PS (upper part) compared to that of a sample of c-Si with the same features of the substrate as the PS sample. In the greyscale, dark shading corresponds to low intensity and light shading corresponds to high intensity. (One milliradian is equivalent to 0.137 momentum au.)

Moreover, the upper part of figure 2 shows a nearly isotropic narrow peak at $\theta = 0$ (of width $\leqslant 2$ mrad) superimposed onto the broad distribution ascribed to annihilation with electrons in c-Si. Figure 3 shows a cut of the central slices along the [100] direction of the 2D-ACAR spectra of PS and c-Si. Measurements at room temperature did not indicate any noticeable change in the shape of the narrow component. As the total volume of the narrow component was less than 1% of the total volume, one could try to extract it from the total distribution by subtracting the c-Si spectrum from the PS spectrum after normalization to the same number of counts. However, the resulting difference was highly anisotropic, indicating that such a subtraction contained a contribution from the bulk. Therefore, it was decided to subtract the fraction of the c-Si spectrum which minimized the anisotropy of the difference spectrum (for $p \geqslant 1.5$ mrad). The anisotropy $A(p_x, p_y)$ considered is defined as

$$A(p_x, p_y) = \rho_{2D}^{2\gamma}(p_x, p_y) - \rho_{2D}^{2\gamma}(\sqrt{p_x^2 + p_y^2})$$

where $\rho_{2D}^{2\gamma}(p_x, p_y)$ is the experimental spectrum and $\rho_{2D}^{2\gamma}(\sqrt{[p_x^2 + p_y^2]})$ represents its angular average [15]. A 62% fraction of the c-Si spectrum yielded the most isotropic difference spectrum, denoted as PS-diff, shown in figure 4. It is difficult to estimate the ratio of the

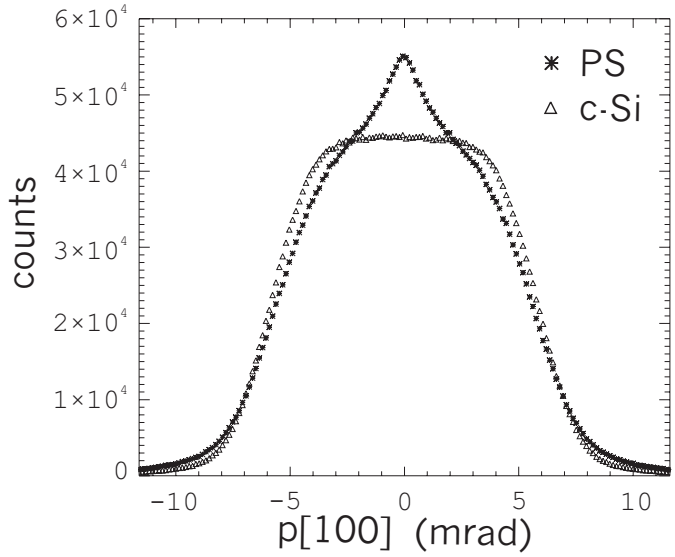

Figure 3. A central slice along the [100] crystal direction of the 2D-ACAR spectra of PS and c-Si. The 2D spectra were normalized to the same number of counts.

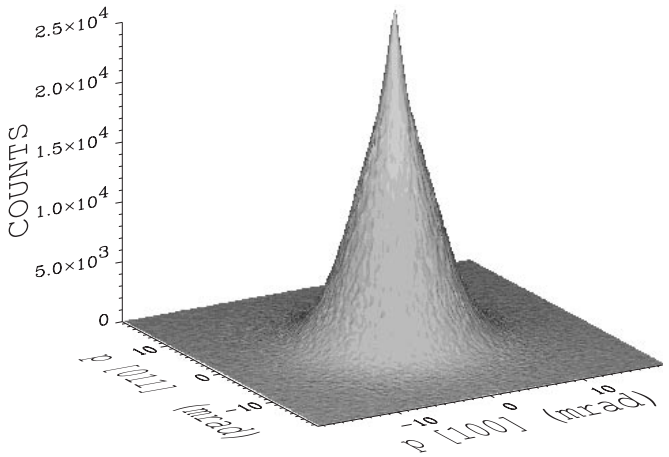

Figure 4. The difference between the 2D-ACAR spectra of PS and 62% of c-Si.

bulk annihilations in the porous layer to those in the Si substrate. According to the empirical expression given in reference [23] for a homogeneous material, the fraction of positrons emitted by a ^{22}Na source stopping within the Si porous layer (having an average density of ∼45% of c-Si) amounts to ∼22%. This would imply that none of the positrons annihilating in the PS layer should contribute to the c-Si part of the spectrum. However, due to the complicated topology of the interconnected pores, equivalent to a multilayered structure, this fraction is probably much higher. Indeed, in the work of reference [11] a PS layer only 0.2 μm thick contributed significantly to the total 2D-ACAR spectrum, showing clearly a narrow component similar to that of figure 3. Interestingly, one could fit the PS-diff spectrum (having 256^2 degrees of freedom) with three two-dimensional Gaussian functions, obtaining a satisfactory reduced

chi squared, $\chi^2/\nu = 3.5$. The value of χ^2/ν, 30 times smaller than that for an analogous fit to the total PS spectrum, indicates that the contribution from annihilations in the bulk was removed from PS-diff, which can then uniquely be ascribed to annihilations in the pores and in defect-like structures present in the nanowires.

The results of the fit are reported in table 2. Figure 5 shows a p_y-slice of the fitting Gaussians and the corresponding slice of the difference spectrum. (The analogous p_x-slices look almost identical to the p_y-slices.) The narrowest Gaussian component (G_3 in table 2) had the same width and intensity, which could be deduced directly from the experimental spectrum (see figure 3). This component and the long lifetime τ_3 indicate Ps formation in the porous layer, whereas the two broader components (G_1 and G_2) and the lifetime τ_2 suggest a momentum and spatial distribution of electrons localized in defects somewhat related to the columnar structures. As the difference spectrum represents ∼38% of the total PS spectrum, the intensity of the narrow component turns out to be approximately 1/4 of the intensity of the third intensity in the lifetime experiment (i) (performed right after the 2D-ACAR experiment) which is fairly consistent with the ratio 3:1 of the statistical weight of ortho-positronium to that of the para-positronium. Final clear-cut evidence of the presence of Ps in the 2D-ACAR spectrum is given by a polarization experiment. It is well known that, owing to the positron helicity at the emission, there is a preferential formation of a singlet (triplet) state of positronium if an external magnetic field is parallel (antiparallel) to the positron spin, with an increase (decrease) of the intensity of the narrow momentum distribution of the centre of mass of para-positronium (the singlet state of Ps). A test for the presence of Ps consists then in taking the difference between one spectrum collected when the magnetic field is parallel to the positron emission direction

Table 2. Parameter values of the three Gaussians fitting the PS-diff part of the 2D-ACAR spectrum of porous Si.

Gaussian	Intensity (%)	FWHM$_{p_x}$ (mrad)	FWHM$_{p_y}$ (mrad)
G_1	71 ± 1	8.40 ± 0.03	8.42 ± 0.03
G_2	28 ± 1	6.24 ± 0.02	6.38 ± 0.02
G_3	1 ± 0.1	1.58 ± 0.01	1.68 ± 0.01

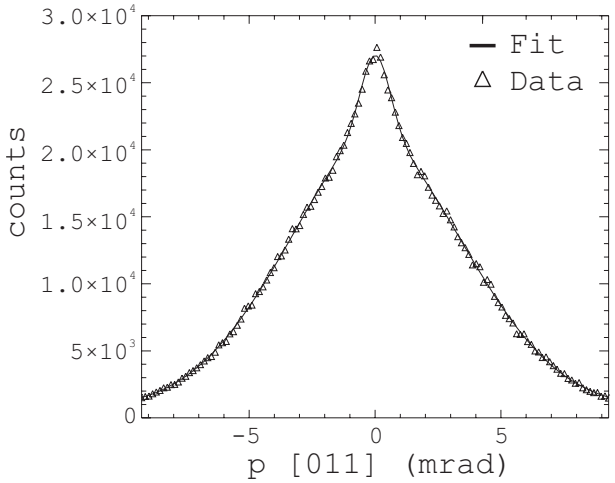

Figure 5. A central slice along the p_y-direction of the PS-diff spectrum shown in figure 4 and the fit with the three 2D Gaussians (continuous line) described in table 2.

and a spectrum with the magnetic field reversed [24]. As the experimental resolution is not altered by these different configurations, such a difference is suited to detecting small amounts of Ps. A separate experiment on quartz, with a 1.95 T polarizing $\boldsymbol{B}$-field, had detected a ∼20% difference in the height of the para-Ps peak. Owing to the small intensity of the hypothetical para-Ps peak, we analysed the spectra with the 1.95 T magnetic field $\boldsymbol{B}$ parallel (antiparallel) to the positron emission in terms of the S-parameter, defined as the fractional area of a fixed central part (here 3.5 mrad wide) to the total 1D momentum-density profile. The 1D profiles were obtained by integrating the 2D-ACAR spectra over a central 1.75 mrad wide region. A difference of eight times the statistical uncertainty between the corresponding S-parameters ($S_{para} = 0.4676 \pm 0.0002$, $S_{antipara} = 0.4660 \pm 0.0003$) indicated that the spectrum obtained with $\boldsymbol{B}$ parallel to the positron emission was narrower than the spectrum obtained with $\boldsymbol{B}$ antiparallel, indicating the presence of Ps. On the other hand, the absence of change in the width of the narrow peak with the temperature indicates that positronium is formed in the voids which characterize the porous layer. Therefore, we utilized the model which calculates the momentum density of the centre of mass of a Ps atom confined in a spherical microvoid developed in reference [25]. As the model was implemented for 1D-ACAR experiments, to estimate the diameter of the void from a slice of the 2D-ACAR spectrum we reduced the number of integrations of the 3D calculated momentum density to one. The equation

$$D_0\ (\text{Å}) = \frac{34.04}{\theta_{1/2}\ (\text{mrad})} \tag{4}$$

provides the resulting numerical relation between the diameter of the hole in Å, D_0, and the full width at half-maximum (FWHM) of the 2D momentum distribution in mrad, $\theta_{1/2}$.

If one inserts in equation (4) the FWHMs of the narrow components shown in table 2 after the deconvolution from the asymmetric experimental resolution (which, in the case of Gaussian functions, consists simply of a subtraction in quadrature), one obtains $D_0 = 2.32 \pm 0.05$ nm and $D_0 = 2.46 \pm 0.05$ nm for the p_x- and p_y-directions, respectively. Therefore, the sizes of the hole in the two directions are almost identical. It was proposed that the pores have preferential propagation along the [100] direction (parallel to p_x), here coinciding with the current direction [26], or, elsewhere [4], that the porous structures be a random network more similar to a sponge. Although our results seem to support the latter hypothesis, one should be aware that a relevant deviation from the straight line in the geometry of the pores would cancel the anisotropy in the width of the positronium peak.

Finally, we discuss the origin of the second lifetime component (τ_2) and of the broad Gaussian components in the PS-diff spectrum (G_1 and G_2 in table 2). Lifetime values similar to or slightly longer than τ_2 were observed in references [7–10]. The small variation of the S-parameter in the polarization experiment and the rather large values of the FWHMs of G_1 and G_2 exclude the possibility that they are related to the momentum density of the centre of mass of Ps. Therefore, they should be due to annihilations of free positrons trapped at defects related to the columnar structures of the porous layers. A rough order-of-magnitude estimate of their concentration C_d can be obtained via the simple trapping model equation [6]:

$$C_d = \frac{I_2(1/\tau_1 - 1/\tau_2)}{\mu_s} \tag{5}$$

where τ_1, τ_2, I_2 and μ_s are the two lifetimes, the second lifetime intensity and the specific positron trapping rate, respectively. Although there is a discrepancy of ∼20% between the intensities for the annihilations in the trapped state obtained from the 2D-ACAR and the lifetime analysis, the major uncertainty in the estimate arises from the knowledge of the specific positron trapping rate, which depends on the nature of the trapping centres. Inserting in equation (5) the value $\mu_s = 10^{15}\ \text{s}^{-1}$, typical of point defects in semiconductors [27], and the lifetimes and

intensities reported in table 1, one obtains defect concentrations spanning between 2×10^{-6} and 6×10^{-7}. Several speculative suggestions as regards the natures of these traps, such as that they may be vacancy-like or silicon:silicon dioxide interfaces, were made [7–9]. The treatments reported as points (ii) and (iii) in section 2 were meant to alter the surface states to some extent. As very little change in the value and intensity of τ_2 was observed, we suggest that such defects are not related to surface states.

As the presence of diffraction spots in the Von Laue experiment should not be regarded as conclusive evidence of a crystalline phase throughout the porous layer, one could ascribe G_1, G_2 and τ_2 to amorphous islands (a-Si), already suggested as sources of PL [5], present in the PS layer. The momentum density in a-Si was measured by He *et al* [17]. In their work they report a FWHM of ∼9.6 mrad, which is significantly larger than the average width of the present PS-diff distribution ($\overline{\text{FWHM}} = 7.7$ mrad). Therefore, there are no experimental grounds for this hypothesis. The possibility that PS-diff is due to an open-volume defect, such as a divacancy, can also be ruled out on the basis of measurements of Tang *et al* [28], who reported a FWHM of ∼9 mrad, i.e. ∼1.3 mrad larger than the average width of PS-diff.

It was recently suggested [29] that undulations in the diameter of the quantum wires could produce localized states for electrons and positrons in the gap between the conduction band and the valence band. The dominant PL channel should then be yielded by recombination for transitions between these localized states. To date, a theory which estimates the positron lifetime and the width of the electron–positron momentum distribution in these localized states is lacking. The typical sizes of the undulations which yield transition energies consistent with the experimental PL results span values between 15 and 40 Å. On the basis of the uncertainty principle, whatever the result of the calculation, the width of the related electron–positron momentum distribution should be smaller than the width of the spectrum ascribed to the divacancy (FWHM ∼ 9 mrad) as measured by Tang *et al* [28], consistent with our current results. It is tempting to ascribe G_1 and G_2 in the PS-diff spectrum and the τ_2-lifetime (although its value seems rather high for such a defect) to this topological trap, as it also provides an explanation for the PL emission during the carrier decay within the localized state.

4. Conclusions

In this work we performed a two-dimensional analysis of 2D-ACAR spectra of a PS sample and of its c-Si substrate. After the subtraction of the anisotropic part of the spectrum we were able to isolate a narrow distribution (clearly visible also in the raw data), attributable to Ps formation, and a broad one, which we attributed to defects inside the columnar structures. From the analysis of the narrow distribution we estimated the average sizes of the pores in the directions parallel and perpendicular to the sample layer but could not confirm a preferential propagation of the pores. The broad distribution of the isotropic part of the spectrum might be related to bulges in the quantum wires causing localization of the electron and positron states.

Acknowledgments

Our thanks to D Ninno for stimulating discussions. One of us (MAM) acknowledges support from an ENEA grant.

References

[1] Lehmann V and Gösele U 1991 *Appl. Phys. Lett.* **58** 856
[2] Canham L T 1990 *Appl. Phys. Lett.* **57** 1046

[3] Moyer P J, Cloninger T L, Gole J L and Bottomley L A 1999 *Phys. Rev.* B **60** 4889
[4] Prokes S M, Glembocki O J, Bermudez V M, Kaplan R, Friederson L E and Searson P C 1992 *Phys. Rev.* B **45** 13 788
[5] Jung K H, Shih S and Kwong D L 1993 *J. Electrochem. Soc.* **140** 3046
[6] West R N 1979 *Positrons in Solids (Springer Topics in Current Physics)* ed P Hautojarvi (Berlin: Springer) p 89
[7] Itoh Y, Murakami H and Kinoshita A 1993 *Appl. Phys. Lett.* **63** 2798
[8] Suzuki R, Mikado T, Ohgaki H, Chiwaki M, Yamazaki T and Kobayashi Y 1994 *Phys. Rev.* B **49** 17 484
[9] Dannefaer S, Wiebe C and Kerr D 1998 *J. Appl. Phys.* **84** 6559
[10] De La Cruz M and Pareja R 1989 *Phys. Status Solidi* a **111** 463
[11] Haung C C, Chang I M, Chen Y F and Tseng P K 1996 *Physica* B **228** 374
[12] Haung C C, Chang I M, Chen Y F and Tseng P K 1998 *Physica* B **245** 9
[13] Berko S 1983 *Proc. Int. Enrico Fermi School of Physics* ed W Brandt and A Dupasquier (Amsterdam: North-Holland) p 64
[14] Mijnarends P E 1983 *Proc. Int. Enrico Fermi School of Physics* ed W Brandt and A Dupasquier (Amsterdam: North-Holland) p 25
[15] West R N 1993 *Proc. Int. Enrico Fermi School of Physics* ed A Dupasquier and A P Mills Jr (Amsterdam: North-Holland) p 75
[16] Ambigapathy R, Manuel A A, Hautojärvi P, Saarinen K and Corbel K 1994 *Phys. Rev.* B **50** 2188
[17] He Y J, Hasegawa M, Lee R, Berko S, Adler D and Jung A L 1986 *Phys. Rev.* B **33** 5924
[18] Cullis A G and Canham L T 1991 *Nature* **353** 335
[19] West R N, Mayers J and Walters P A 1981 *J. Phys. E: Sci. Instrum.* **14** 478
[20] Kirkegaard P and Eldrup M 1981 *Comput. Phys. Commun.* **23** 307
[21] Chiba T and Akahane T 1988 *Positron Annihilation* ed L Dorikens-Vanpraet, M Dorikens and D Segers (Singapore: World Scientific) p 674
[22] Tanigawa S, Uedono A, Wei L and Suzuki R 1993 *Proc. Int. Enrico Fermi School of Physics* ed A Dupasquier and A P Mills Jr (Amsterdam: North-Holland) p 729
[23] Brandt W and Paulin P 1977 *Phys. Rev.* B **15** 2511
[24] Page L A and Heinberg M 1957 *Phys. Rev.* **106** 1220
[25] Nakanishi H and Jean Y C 1988 *Positron and Positronium Chemistry* ed D M Schrader and Y C Jean (Amsterdam: Elsevier) p 159
[26] Chuang S F, Collins S D and Smith R L 1989 *Appl. Phys. Lett.* **55** 675
[27] Krause-Rehberg R and Leipner H S 1999 *Positron Annihilation in Semiconductor Defect Studies* (Berlin: Springer) p 103
[28] Tang Z, Hasegawa M, Chiba T, Saito M, Kawasuso A, Li Z Q, Fu R T, Akahane T, Kawazoe Y and Yamaguchi S 1997 *Phys. Rev. Lett.* **78** 2236
[29] Ninno D, Iadonisi G and Buonocore F 1999 *Solid State Commun.* **112** 521